The TCM Prescription Yi-Fei-Jie-Du-Tang Inhibit Invasive Migration and EMT of Lung Cancer Cells by Activating Autophagy

Shanshan Wang
Yangzhou University School of Medicine: Yangzhou University Medical college
Zaichuan Wang
Yangzhou University
Yinqiu Wu
Yangzhou University
Chao Hou
Yangzhou University
Qingyin Wang
Yangzhou University School of Medicine: Yangzhou University Medical college
Yongjian Wu
Yangzhou University School of Medicine: Yangzhou University Medical college
Chao Qian
Yangzhou University School of Medicine: Yangzhou University Medical college
Xiaochun Zhang (ceiq@sina.com)
Yangzhou Hospital of Traditional Chinese Medicine affliated with Nanjing University of Chinese Medicine

---

Research

Keywords: Yi-Fei-Jie-Du-Tang, FAT4, autophagy, epithelial-mesenchymal transition, non-small cell lung cancer

Posted Date: October 12th, 2021

DOI: https://doi.org/10.21203/rs.3.rs-915906/v1

Version of Record: A version of this preprint was published at Evidence-Based Complementary and Alternative Medicine on January 29th, 2022. See the published version at

https://doi.org/10.1155/2022/9160616.

Abstract

Objective

Non-small cell lung cancer (NSCLC) is a serious threat to people's health. This study aims to assess the antitumor effect of Yi-Fei-Jie-Du-Tang (YFJDT) on NSCLC,which is an empirical formula from Professor Zhongying Zhou,and the underlying mechanisms.

Methods

In the present study, we determined the possible effects and potential mechanisms of YFJDT on an A549 cell tumor-bearing nude mice model and A549 cell model in vitro. Tumor-bearing mice were treated with YFJDT and tumors were measured during the experiment, and tumor tissues were collected at the end of the experiment to assess the levels of autophagy and epithelial-mesenchymal transition (EMT)-related proteins.

Results

The results showed that YFJDT treatment reduced tumor volume and mass, increased the expression of the autophagy marker LC3 and inhibited EMT-related proteins compared to the model group.Cell survival was reduced in the YFJDT-treated group compared to the model group, and YFJDT also reduced the migration and invasion ability of A549 cells in a dose-dependent manner. Western blotting detected that YFJDT also upregulated FAT4 in tumor tissue and A549 cells and downregulated the expression of Vimentin. Meanwhile, apoptosis in both tissues and cells was greatly increased after YFJDT treatment. We further interfered with FAT4 expression in cells and found that the inhibitory effect of YFJDT on EMT was reversed, indicating that YFJDT affects EMT by regulating FAT4 expression.

Conclusion

Taken together, results of this study suggested that the inhibitory effect of YFJDT on EMT in lung cancer tumors is through upregulating FAT4, promoting autophagy and thus inhibiting EMT in cancer cells.

Introduction

Lung cancer is currently one of the major malignant tumor threatening human health, with the highest incidence and mortality rate [1]. Non-small cell lung cancer (NSCLC) is the most predominate type of lung cancer, and metastasis is its malignant feature and an important factor in patient survival and prognosis [2; 3]. How to inhibit metastasis is a key breakthrough tool that promote the prognosis of lung cancer patient. Epithelial-mesenchymal transition (EMT) takes part in the invasion and metastasis of lung cancer and plays and important role in it [4; 5]. Recent researches shows that autophagy affects the invasion and metastasis of tumor cells by regulating EMT [6; 7]. Thus, modulation of autophagy to inhibit the development of tumor has become a new direction in tumor therapy.

Yi-Fei-Jie-Du-Tang is an traditional Chinese medicine formula to treat Non-small cell lung cancer (NSCLC),which contains Chinese medical plants, namely, *Glehnia lit-toralis F.Schmidt ex Miq. (Beishashen), Ophiopogon japonicus□L. f□ Ker-GawL (Maidong), Pseudostellaria heterophylla (Miq.)Pax ex Pax et Hoffm. (Taizishen), Euphorbia helioscopia L., (Zeqi), Asarum sagittarioides C. F. Liang. (Shancigu), Sarcandra glabra (Thunb.) Nakai. (Zhongjiefeng), Ranunculus ternatus Thunb. (Maozhuacao), Baijiangcan, Oldenlandia diffusa (Willd) Roxb. (Baihuasheshecao) and Agrimonia pilosa Ledeb. (Xianhecao).*The formula was created by Professor Zhongying Zhou, a National Chinese Medical Science Master and a famous Traditional Chinese Medicine (TCM) expert, combining the etiology of malignant tumours and his many years of clinical experience[8]. In this decoction, Baishashen and Maidong nourish Yin and clear the lung, Taizishen benefits Qi and nourishes Yin, Zeqi, Shancigu and Maozhuacao dissolve phlegm and detoxify nodules, Baijiangcan dispels wind and phlegm, subdues swelling and disperses nodules, Hedyotis diffusa clear heat and detoxify the lung, and Xianhecao nourishes deficiency and detoxifies the lung. Modern pharmacological studies have shown that all the medicines in this formula have certain anti-tumour effects [9; 10].

The results of our previous study showed that Yi-Fei-Jie-Du-Tang could inhibit the invasion, migration and EMT of A549 cells induced by hypoxia [8]. However, it is not clear whether the inhibitory effect of Yi-Fei-Jie-Du-Tang on hypoxia-induced A549 cells invasion, migration and EMT is related to cell autophagy and the mechanism involved. Therefore, this study aims to investigate the molecular mechanism of the inhibitory effect of Yi-Fei-Jie-Du-Tang on the invasion and migration of lung cancer cells *in vitro* and *in vivo* by applying modern molecular biology techniques under the guidance of Chinese medicine theory and taking the autophagy pathway as the entry point. The study will provide a laboratory basis for the clinical application and development of Yi-Fei-Jie-Du-Tang.

Materials And Methods

Preparation and component analysis of Yi-Fei-Jie-Du-Tang

Yi-Fei-Jie-Du-Tang is composed of 12g of Beishashen, 10g of Maidong, 12g of Taizishen, 12g of Shancigu, 15g of Zeqi, 20g of Maozhuacao, 20g of Zhongjiefeng, 15g of Xianhecao, 10g of Baijiangcan 20g of Baihuasheshecao.The herbs were purchased from the Chinese pharmacy of Yangzhou Hospital of Traditional Chinese Medicine affliated with Nanjing University of Chinese Medicine.The criteria for identifying the quality of the herbs used were in accordance with the 2005 edition of the Chinese Pharmacopoeia (Chinese Pharmacopoeia Commission, Pharmacopoeia of the People's Republic of China, Beijing: People's Medical Publishing House; 2005). Prior to their use in experiments, the herbs were tested for heavy metals, microbial contamination, and residual pesticides; all results met the safety standards in China.Laboratory personnel were blinded to the identity of the herbs. A trained technician prepared the decoction according to a standardized procedure. The herbs were steeped in double-distilled water for 30min, boiled over high heat and then decocted over low heat for 30min, then further concentrated by decoction over low heat for 30min, microwave vacuum dried and autoclaved. The herbs used in the experiments were purchased and prepared at one time, then packed and stored in the

refrigerator. The main components of Yi-Fei-Jie-Du-Tang were analyzed using high performance liquid chromatography (HPLC) analysis. Standards were purchased from Macklin Inc.

Antibodies

The primary antibodies used in this study included MMP2 (40994, CST), MMP9 (13667, CST), E-cadherin (14472, CST), β-cadherin (8480, CST), Vimentin (5741, CST), Twist1 (ab50887, abcam), LC3 II/I (12741S, CST), p62 (AF5384, Affinity), PI3K (AF6241, Affinity), p-PI3K (ab32089, abcam), Akt (4691, CST), p-Akt (5536, CST), p-mTOR (9271, CST), mTOR (2983, CST), GSK3β (5676, CST), p-GSK3β (9322, CST) and Tubulin (5335, CST).

Tumor-carrying mouse model and drug treatment

BALB/c male nude mice (20~24g) were purchased from Jiangsu Provincial Center for Disease Control and Prevention (Animal license number: SYXK(Su)2017-0030, Jiangsu, China). Naked mice were housed in an IVC environment with free access to feed and pure water. Human NSCLC A549 cells were purchased from the Cell Bank of the Chinese Academy of Sciences of Shanghai. Cells were cultured in RPMI-1640 medium in an incubator with a CO_2 concentration of 5% at 37°C.

A549 cells at logarithmic growth stage were made into a single cell suspension with a cell density of 1×10^7cells/mL and 0.2mL of this suspension was inoculated into the right axillary subcutis of nude mice. A tumor-bearing nude mouse model was successfully developed when the tumor volume of the nude mouse reached 100-150 mm^3.

Mice were randomly divided into five groups: Model group, L-YFJDT group (6.5g/kg/d YFJDT), M-YFJDT group (13g/kg/d YFJDT), H-YFJDT group (26g/kg/d YFJDT and Gefitinib group (7.5mg/kg/d Gefitinib). In the Model group, the same amount of saline was administered by gavage. The longest diameter and the wide diameter perpendicular to the tumor of the nude mice were measured every 3 days from the first day of administration and the tumor volume was calculated. After 21 days of treatment, nude mice were euthanized and tumor were weighed to calculate the inhibition rate of the YFJDT on the tumors.

Immunohistochemical detection

The tumours were fixed in 4% formaldehyde and embedded in paraffin and cut into 4 μm thick sections. Sections were incubated with FAT4 antibody (PA5-72970 Invitrogen) for 2 h and incubated with Goat Anti-Rabbit IgG H&L (Alexa Fluor 488) (ab150077, abcam) for 30 min at room temperature. FAT4 expression rates were determined by ImageJ software.

Cell culture and YFJDT treatment

A549 cells were cultured in RPMI 1640 medium containing 10% fetal bovine serum and 1% double antibiotics in a 5% CO_2 incubator at 37°C. The cells were grown in logarithmic growth phase with a cell count of 5×10^5 to 1×10^6 /mL.

YFJDT was administered to SD rats by gavage (according to the clinical dosage × 6). Rats in the low dose group were given 1.7g/kg/d by gavage, rats in the middle dose group 3.4g/kg/d, rats in the high dose group 6.8g/kg/d, and rats in the blank control group were given an equal volume of distilled water. Blood was collected from the abdominal aorta 1 h after the last YFJDT gavage, and the serum was separated after fasting for 12 h before the last YFJDT gavage. The serum was filtered through a 0.22 microporous filter, sterilized and divided and stored at -80°C in the refrigerator[11]. The cells were incubated with different concentrations of YFJDT-containing serum for 24 h. The cell proliferation was detected by MTT, and the three drug concentrations that inhibited cell proliferation were screened out.

Cells were divided into four groups: model group, L-YFJDT group, M-YFJDT group and H-YFJDT group. Cells in each group were incubated with the corresponding concentrations of YFJDT-containing serum for 24 h respectively to verify the effectiveness of the above concentrations of YFJDT in inhibiting the proliferation of cancer cells at different time points.

Cell viability detection

The A549 cells were incubated in 5% CO2 at 37°C until the cells were plastered with the corresponding concentration of YFJDT-containing serum, and incubated for 24 h. After that, 20 uL of MTT solution was added to each well and incubated for 4 h. Then 150 uL of dimethyl sulfoxide was added to each well and shaken at low speed for 10 min to dissolve the crystalline material, and the absorbance value of each well was measured at OD 490 nm.

Cellular invasiveness assay

The matrix gel was left overnight at 4°C. The matrix gel was diluted 1:8 and wrapped around the upper chamber surface of the membrane at the bottom of the transwell, air-dried and the residual culture fluid in the chamber was aspirated. The YFJDT-containing serum treated cell suspension was adjusted to a cell density of 2×10^5 cells/mL with serum-free cell culture medium. 200 uL of cell suspension was added to each well of the upper chamber and 600 μL of culture medium containing 10% fetal bovine serum was added to the lower chamber. The plates were incubated in an incubator at 37°C for 24 h. The chambers were removed and rinsed twice with PBS buffer. The cells on top of the chambers were carefully wiped off with a cotton swab, and the cells on the bottom of the chambers were fixed with 4% paraformaldehyde for 20 min and stained with 0.1% crystal violet for 15 min.

The cell density was adjusted to about 6×10^5 cells/mL, and the cell layer at the bottom of the plate was quickly scratched with a gun along the vertical line of the sterilized ruler, and the 6-well plate was rinsed twice with PBS solution after scratching. After 24h of incubation with YFJDT-containing serum, the extent of cell healing was observed under the microscope and photographed, and the migration rate was calculated according to the healing of the scratch. Migration rate=[(distance migrated by the intervention group/distance migrated by the control group)-1] × 100%

GFP-LC3 co-localization assay with lysosomes

A549 cells stably transfected with GFP-LC3 plasmid at logarithmic growth stage were subjected to hypoxia induction after 80% fusion, and then incubated for 24 h with the addition of YFJDT containing serum and a blank control. After incubation, the wells were incubated with 50 nM LysoTracker Red DND-99 (L8010, Solarbio, China) for 30 min at 37°C. The wells were washed with PBS and fixed for 1 min.

Western blot analysis

Equal amounts of protein were separated by SDS-PAGE 12% and transferred onto PVDF membranes. After blocking with 5% skimmed milk for 2 h, the membranes were incubated sequentially with primary antibody and HRP-conjugated secondary antibody. The final protein bands were observed after color development with ECL reagents. The intensity of each sample was determined using ImageJ software.

Apoptosis detection by flow cytometry

Cells were collected after digestion with EDTA-free trypsin and washed twice with pre-cooled PBS to turn them into a suspension of 5×10^6 cells/mL. YF488-Annexin V (YF®488-Annexin V and PI Apoptosis Kit, US EVERBRIG, China) and 5 μL of PI working solution were added to each tube and incubated on ice for 10-15 min at room temperature, protected from light. 400 μL of PBS was added to each tube and the apoptotic cells were examined by flow cytometry as soon as possible. The fluorescence emission spectrum was detected at 530 nm (FITC channel) and the PI channel emission spectrum at approximately 617 nm.

Quantitative real-time polymerase chain reaction

Mixed sample RNA, specific primers, 2× FastKing One Step RT-PCR MasterMix and RNaseFree ddH2O were placed into the real-time PCR instrument using the FastKing One Step RT-PCR kit (Tiangen, China) according to the manufacturer's instructions. The mRNA expression levels of E-cadherin, Vimentin and Twist1 were measured using GAPDH as an internal reference gene. The primers used were as follows: E-cadherin-F, TGGACCGAGAGAGTTTCCCT and E-cadherin-R, CAAAATCCAAGCCCGTGGTG; Vimentin-F, TCCGCACATTCGAGCAAAGA and Vimentin-R ATTCAAGTCTCAGCGGGCTC; Twist1-F, CCGTGGACAGTGATTCCCAG and Twist1-R, CCTTTCAGTGGCTGATTGGC; GAPDH-F, CTGGGCTACACTGAGCACC and GAPDH-R, AAGTGGTCGTTGAGGGCAATG.

Statistical analysis

The data were analyzed using Prisim 8.02. Comparisons between groups were made using the Student’s t-test, and values from three independent experiments are expressed as mean ± SD. Differences were considered statistically significant at *$p<0.05$ and **$p<0.01$.

Results

HPLC analysis of Yi-Fei-Jie-Du-Tang

HPLC analysis was performed to evaluate the major component of YFJDT. As shown in Figure 1A and B, seven key compounds in YFJDT including chlorogenic acid, salicylic acid, militarine, hyperoside, rutinum, wogonin and psoralen were determined by external standard method. The contents of these compounds were 0.857 mg/g, 0.529 mg/g, 0.097 mg/g, 1.024 mg/g, 0.113 mg/g, 0.079 mg/g, 0.015 mg/g, respectively.

YFJDT reduces the volume and weight of tumor in mice

To explore whether YFJDT has anti-tumor effects in mice, YFJDT was gavaged into tumor-bearing mice and the tumors were photographed and recorded, as shown in Figure 2A. The volume and weight of the tumors were also recorded and YFJDT was found to significantly reduce the volume and weight of the tumors ($p<0.05$, Figure 2B and C). FAT4 has been shown to inhibit epithelial to mesenchymal transition (EMT) and to function as a tumor suppressor [12]. YFJDT treatment increased the content of FAT4 in the lung tumor tissue compared to the Control group (Figure 2D). In Figure 2F, the mRNA expression of E-cadherin was increased and the mRNA expressions of Vimentin and Twist1 were decreased with the treatment of YFJDT. With reference to previous studies, we performed apoptosis assays on tumor tissues and found that the proportion of apoptosis in the tumors of mice in the YFJDT-treated group was greatly increased relative to the model group ($p<0.05$, Figures 2E).

YFJDT promotes autophagy related proteins and inhibits migration proteins

The above results indicated that YFJDT had an inhibitory effect on lung cancer tumors. This was further verified using a western blot method as shown in Figures 3A and B. The results showed that treatment with YFJDT increased the expressions of LC3 II/I, E-cadherin and decreased the expression of MMP2, MMP9, β-cadherin, Vimentin, Twist1 and p62, while YFJDT also decreased the phosphorylated forms of PI3K, Akt, mTOR and GSK3β, but not PI3K, Akt, mTOR and GSK3β per se.

YFJDT-containing serum inhibits the proliferation of A549 cells

Cell proliferation was assayed at different time and it was found that the cell proliferation capacity of the administered group decreased significantly with increasing time compared to the Model group in a dose-dependent manner ($p<0.05$, Figures 4A). The efficacy of YFJDT was further validated when we examined the invasive and migratory capacity of YFJDT-treated A549 cells using the transwell assay and cell scratch assay. The transwell migration assay data showed that YFJDT significantly inhibited cell invasion of A549 cells and that higher concentration of YFJDT containing serum had a better inhibitory effect than lower concentrations ($p<0.05$, Figure 4B). Similarly, the ability of cells to migrate was statistically significantly altered by YFJDT inhibition ($p<0.05$, Figure 4C).

YFJDT increases the expressions of LC3 and FAT4 and the ratio of apoptosis

To determine whether the decreased viability of A549 cells was associated with autophagy, we examined LC3 to determine the autophagy status of YFJDT-containing serum treated cells. In A549 normal cells, GFP-LC3 fluorescence was mostly diffuse, with bright green fluorescent spots appearing with increasing

drug concentrations, and co-localization of GFP-LC3B with lysosomes increased in a dose-dependent manner with increasing drug concentrations (Figure 5A). Further detection of apoptosis by flow assay yielded similar results, with higher rates of apoptosis in the YFJDT-treated groups compared to the control group (Figure 5B). Interestingly, the contents of FAT4 of YFJDT groups also increased obviously, in particular, the highest expression of FAT4 was found in the concentration of YFJDT ($p<0.05$, Figure 5C). In Figure 5D, the mRNA expression of E-cadherin was increased and the mRNA expressions of Vimentin and Twist1 were decreased with the treatment of YFJDT.

YFJDT promotes autophagy related proteins and inhibits migration proteins *in vitro*

Considering the effects of YFJDT on autophagy and migration on A549 cells, the expressions of MMP2, MMP9, E-cadherin, β-catenin, Vimentin, Twist1, LC3 II/I, p62, p-PI3K, PI3K, Akt, p-Akt, mTOR, p-mTOR, GSK3β and p-GSK3β were verified by western blot as shown in Figures 6A and B. The results showed that treatment with YFJDT increased the expressions of LC3 II/I, E-cadherin and decreased the expression of MMP2, MMP9, β-cadherin, Vimentin, Twist1 and p62, while YFJDT also decreased the phosphorylated forms of PI3K, Akt, mTOR and GSK3β, but not PI3K, Akt, mTOR and GSK3β per se.

Si-FAT4 reduces the inhibition of YFJDT on the autophagy and migration of A549 cells

We used FAT4 si-RNA to successfully interfered the expression of FAT4 (Figure 7A). At the same time, the decreased cell viability induced by YFJDT compared to model group has been enhanced in cell treated with the FAT4 si-RNA (Figure 7B). Besides these, the YFJDT-induced increase in LC3 expression and the decrease in p-PI3K, Twist1 and β-catenin expression were all reversed (Figure 7C).

Discussion

Infiltrative growth and distant metastasis are important biological properties of cancer cells[13]. 90% of cancer deaths are due to migration, and inhibiting tumor migration can slow down tumor progression [14; 15]. Similarly, the majority of NSCLC patients die not due to the primary lesion but due to the consequent advanced metastasis [16]. EMT is the biological process by which epithelial cells are transformed into cells with a mesenchymal phenotype through a specific procedure, mainly in the form of an Ecadherin-dominated to Vimentin-dominated cytoskeleton[17]. EMT causes epithelial cells to lose their original cell polarity, disrupting the tight junctions of the cell basement membrane and acquiring a high invasive and migratory capacity [18; 19]. Therefore, EMT is an important reason for the enhanced invasive and migratory capacity of epithelial-derived cancer cells.

In our previous study, we observed that YFJDT exhibited interesting anti-tumour activity against A549 cells [20]. Solid tumor bodies of tumor-bearing mice were exposed to a hypoxic environment, which led to the occurrence of EMT in tumor cells [21]. EMT allows cancer cells to survive independently of the primary tumor site and these cells may exhibit some degree of sensitivity to autophagy. Based on the important role of tumor cell autophagy in their invasive migration, EMT, and the results of our previous study, we explored whether cellular autophagy is involved in the EMT process and how YFJDT affects this

role through the autophagic pathway. To this end, the expressions of autophagy and EMT-related proteins was measured before and after YFJDT treatment. In in vivo experiments, YFJDT reduced the volume and mass of the tumor bodies (Figure 2A-C). Western blot analysis showed that YFJDT treatment led to an increase in LC3 and E-cadherin and a significant decrease in p62 and E-cadherin, indicating that YFJDT treatment increases autophagy levels and decreases EMT (Figure 3 and Figure 6). These results demonstrate that YFJDT can inhibit the EMT process in mouse lung cancer tumors, while the exact mechanism needs to be further explored.

FAT4 is a tumor suppressor and previous studies have shown that FAT4 can inhibit EMT and the proliferation of gastric and rectal cancer cells [12; 22]. We found that treatment with YFJDT increased FAT4, accompanied by increased apoptosis, autophagy and inhibition of EMT, both in tumor-bearing mice and in A549 cells, which is similar to previous finding [12]. Twist1, an important mediator downstream of β-catenin, induces an E-cadherin-mediated decrease in cell-cell adhesion and promotes EMT [23]. The inhibition of EMT by FAT4 may be mediated by levels of β-catenin followed by downregulation of Twist1 expression, as confirmed in previous gastric cancer study [22].

Cancer cells are exposed to more environmental and intrinsic metabolic stresses than normal cells and may be significantly more dependent on autophagy [24]. In the early stages of cancer cell metastasis, autophagy can inhibit metastasis [25]. Both in vivo and in vitro, increased FAT4 expression was accompanied by increased LC3 expression, as well as decreased p62. LC3 is a biomarker of autophagy, and the accumulation of p62 reduces autophagy, suggesting that increased FAT4 is accompanied by increased autophagy [24]. Upregulation of autophagy may limit EMT by increasing the instability of key EMT proteins, such as the Twist1 protein [26; 27]. We further interfered with FAT4 with FAT4-siRNA and found that the initial inhibition of EMT by YFJDT was blocked in A549 cells (Figure 8).

Conclusion

We demonstrated for the first time that YFJDT could activate autophagy via the FAT4, thereby inducing apoptosis and inhibiting EMT and invasion and migration of A549 cells, and the specific mechanism is illustrated in Figure 8.

Abbreviations

NSCLC：Non-small cell lung cancer

YFJDT：Yi-Fei-Jie-Du-Tang

EMT：epithelial-mesenchymal transition

TCM：Traditional Chinese Medicine

HPLC：high performance liquid chromatography

Declarations

Data Sharing Statement

The datasets used and/or analyzed during the current study available from the corresponding author on reasonable request.

Ethics Approval and Consent to Participate

The animal study was reviewed and approved by the Institutional Animal Care and Use Committee of Yangzhou University. All experimental animal procedures were performed in compliance with the institutional ethics requirements. Written informed consent was obtained from all participants.

Consent for Publication

All participants signed a document of informed consent.

Acknowledgments

Not applicable.

Author contributions

SSW and XCZ designed the study. ZCW, YQW, SSW and CH performed the experiments. QYW and CQ completed the literature research. ZCW, YQW and YJW performed the statistical analysis.SSW and ZCW prepared the manuscript. All authors read and approved the submitted version.

Funding

The present study was supported by Natural Science Foundation of Jiangsu Provincial of China (BK20180278).And Construction Project of the third batch inheritance studios of famous traditional Chinese medicine experts in Jiangsu Province.

Competing interests

The authors declare that they have no competing interests.

References

[1]Siegel R, Miller, K, Jemal, A. Cancer statistics. *CA Cancer J. Clin.* 2020; 70: 7–30. doi: 10.3322/caac.21590.

[2]Charles S, Dela, C, Tanoue, LT, et al. Lung Cancer: Epidemiology, Etiology, and Prevention. *Clin. Chest. Med.* 2011; 32: 605-644. doi: 10.1016/j.ccm.2011.09.001.

[3]Califano R, Kerr, K, Morgan, RD, et al. Immune Checkpoint Blockade: A New Era for Non-Small Cell Lung Cancer. *Curr. Oncol. Rep.* 2016; 18: 59. doi: 10.1007/s11912-016-0544-7.

[4]Yang L, Chen, P, Zu, L, et al. MicroRNA-338-3p suppresses metastasis of lung cancer cells by targeting the EMT regulator Sox4. *Am. J. Cancer. Res.* 2016; 6: 127-140. PMID: 27508100.

[5]Mittal V. Epithelial Mesenchymal Transition in Aggressive Lung Cancers. *Adv. Exp. Med. Biol.* 2016; 890: 37-56. doi: 10.1007/978-3-319-24932-2_3.

[6]Choi K. Autophagy and cancer. *Exp. Mol. Med.* 2012; 44: 109-120. doi: 10.3858/emm.2012.44.2.033.

[7]Babaei G, Aziz, SG-G, Jaghi, NZZ. EMT, cancer stem cells and autophagy: The three main axes of metastasis. *Biomed. Pharmacother.* 2021; 133: 110909. doi: 10.1016/j.biopha.2020.110909.

[8]Wang SS, Zhao, XX, Guo, LZ. Intervention Effect and Mechanism of Yifei Jiedu Decoction in Invasion and Metastasis of Lung Cancer Cell A549. *Chin J ExpTradit Med Formulae.* 2017; 23: 108-113.

[9]Woyengo TA, Ramprasath, VR, Jones, P. Anticancer effects of phytosterols. *Eur. J. Clin. Nut.* 2009; 63: 813-820. doi: 10.1038/ejcn.2009.29.

[10]Fan Y, Ma, Z, Zhao, L, et al. Anti-tumor activities and mechanisms of Traditional Chinese medicines formulas: A review. *Biomed. Pharmacother. .* 2020; 132: 110820. doi: 10.1016/j.biopha.2020.110820.

[11]Cheng Z, Zhang, J, Deng, W, et al. Bushen Yijing Decoction (BSYJ) exerts an anti-systemic sclerosis effect via regulating MicroRNA-26a /FLI1 axis. . *Bioengineered.* 2021; 12: 1212-1225. doi: 10.1080/21655979.2021.1907128.

[12]Wei R, Xiao, Y, Song, Y, et al. FAT4 regulates the EMT and autophagy in colorectal cancer cells in part via the PI3K-AKT signaling axis. *J. Exp. Clin. Cancer Res.* 2019; 38. doi: 10.1186/s13046-019-1043-0.

[13]Liu D, Feng, X, Wu, X. Tumor suppressor in lung cancer(TSLC 1),a novel tumor suppressor gene,is implicated in the regulation of proliferation,invasion,cell cycle,apoptosis,and tumorigenicity in cutaneous squamous cell carcinoma. *Tumor Biol.* 2013; 34: 3773-3783. doi: 10.1007/s13277-013-0961-2.

[14]Ferlay J, Colombet, M, Soerjomataram, I, et al. Estimating the global cancer incidence and mortality in 2018: GLOBOCAN sources and methods. *Int. J. Cancer.* 2019; 144: 1941–1953. . doi: 10.1002/ijc.31937.

[15]Paul CD, Mistriotis, P, Konstantopoulos, K. Cancer cell motility: lessons from migration in confined spaces. *Nat. Rev. Cancer.* 2017; 17: 131–140. doi: 10.1038/nrc.2016.123.

[16]Deng X, Ma, Q, Zhang, B. Migration-stimulating factor(MSF)is over-expressed in non-small cell lung cancer and promotes cell migration and invasion in A549 cells over-expressing MSI. *Exp. Cell. Res.* 2013; 319: 2545-2553. doi: 10.1016/j.yexcr.2013.05.016.

[17]Samatov TR, Tonevitsky, AG, Schumacher, U. Epithelial-mesenchymal transition: focus on metastatic cascade, alternative splicing, non-coding RNAs and modulating compounds. *Mol. Cancer.* 2013; 12: 107. doi: 10.1186/1476-4598-12-107.

[18]Chaffer CL, Weinberg, RA. A perspective on cancer cell metastasis. *Science.* 2011; 331: 1559-1564. doi: 10.1126/science.1203543.

[19]Tam WL, Weinberg, RA. The epigenetics of epithelialmesenchymal plasticity in cancer. *Nat. Med.* 2013; 19: 1438-1449. doi: 10.1038/nm.3336.

[20]Wang SS, Zhao, XX, Guo, LZ. Intervention Effect and Mechanism of Yifei Jiedu Decoction in Invasion and Metastasis of Lung Cancer Cell A549. *Chin. J. Exp. Tradit. Med. Formulae.* 2017; 23: 108-113. doi: 10.7501/j.issn.0253-2670.2018.04.019.

[21]Mathew R, Karantzawadsworth, V, White, E. Role of autophagy in cancer. *Nat. Rev. Cancer.* 2007; 7: 961-967. doi: 10.1038/nrc2254.

[22]Egan D, Chun, MH, Vamos, M, et al. Small molecule inhibition of the autophagy kinase ULK1 and identification of ULK1 substrates. *Mol. Cell.* 2015; 99: 285–297. doi: 10.1016/j.molcel.2015.05.031.

[23]Shamir ER, Pappalardo, E, Jorgens, DM, et al. Twist1-induced dissemination preserves epithelial identity and requires E-cadherin. *J. Cell Biol. .* 2014; 204: 839–856. doi: 10.1083/jcb.201306088.

[24]Kroemer G, Mariño, G, Levine, B. Autophagy and the integrated stress response. *Mol. Cell.* 2010; 40: 280–293. doi: 10.1016/j.molcel.2010.09.023.

[25]Ghader Babaei, Shiva Gholizadeh-Ghaleh Aziz, Nasrin Zare Zavieyh Jaghi. EMT, cancer stem cells and autophagy; The three main axes of metastasis. *Biomed Pharmacoth* 2021; 133: 110909.

[26]Gugnoni M, Sancisi, V, Gandolfi, G, et al. Cadherin-6 promotes EMT and cancer metastasis by restraining autophagy. *Oncogene. .* 2016; 36: 667-677. doi: 10.1038/onc.2016.237.

[27]Qiang L, He, Y. Autophagy deficiency stabilizes TWIST1 to promote epithelial-mesenchymal transition. *Autophagy.* 2014; 10: 1864–1865. doi: 10.4161/auto.32171.

Figures

Fig. 1

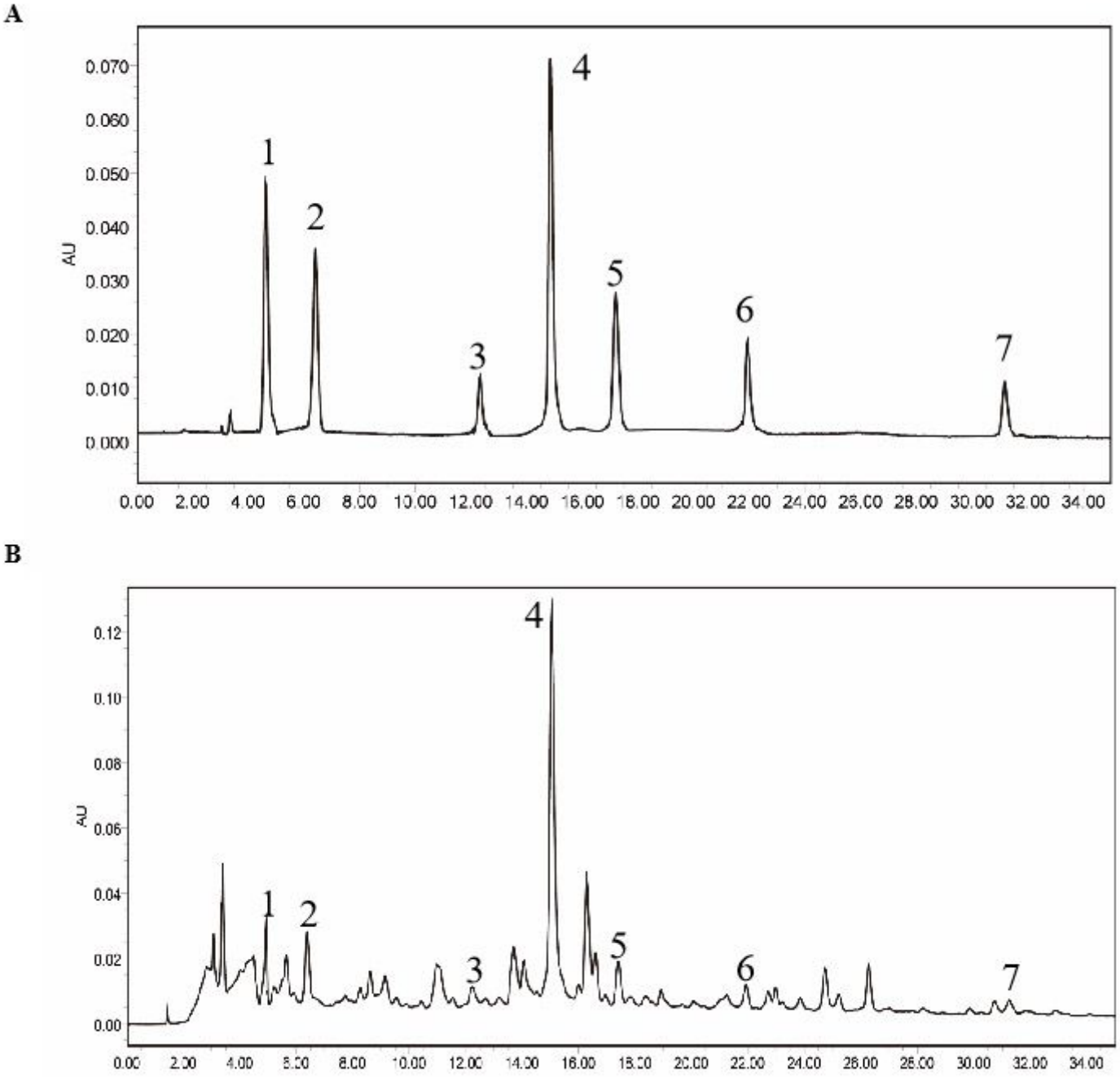

Figure 1

Representative HPLC chromatograms of YFJDT extracts and external standard mix. (A) Chromatographic analysis of 7 standards. (B) Average chromatographic analysis of YFJDT. The 7 common peaks were labelled. 1: chlorogenic acid, 0.857 mg/g; 2: salicylic acid, 0.529 mg/g; 3: militarine, 0. 097 mg/g; 4: hyperoside, 1.024 mg/g; 5: rutinum, 0.113 mg/g; 6: wogonin, 0.079 mg/g; 7: psoralen, 0.015 mg/g.

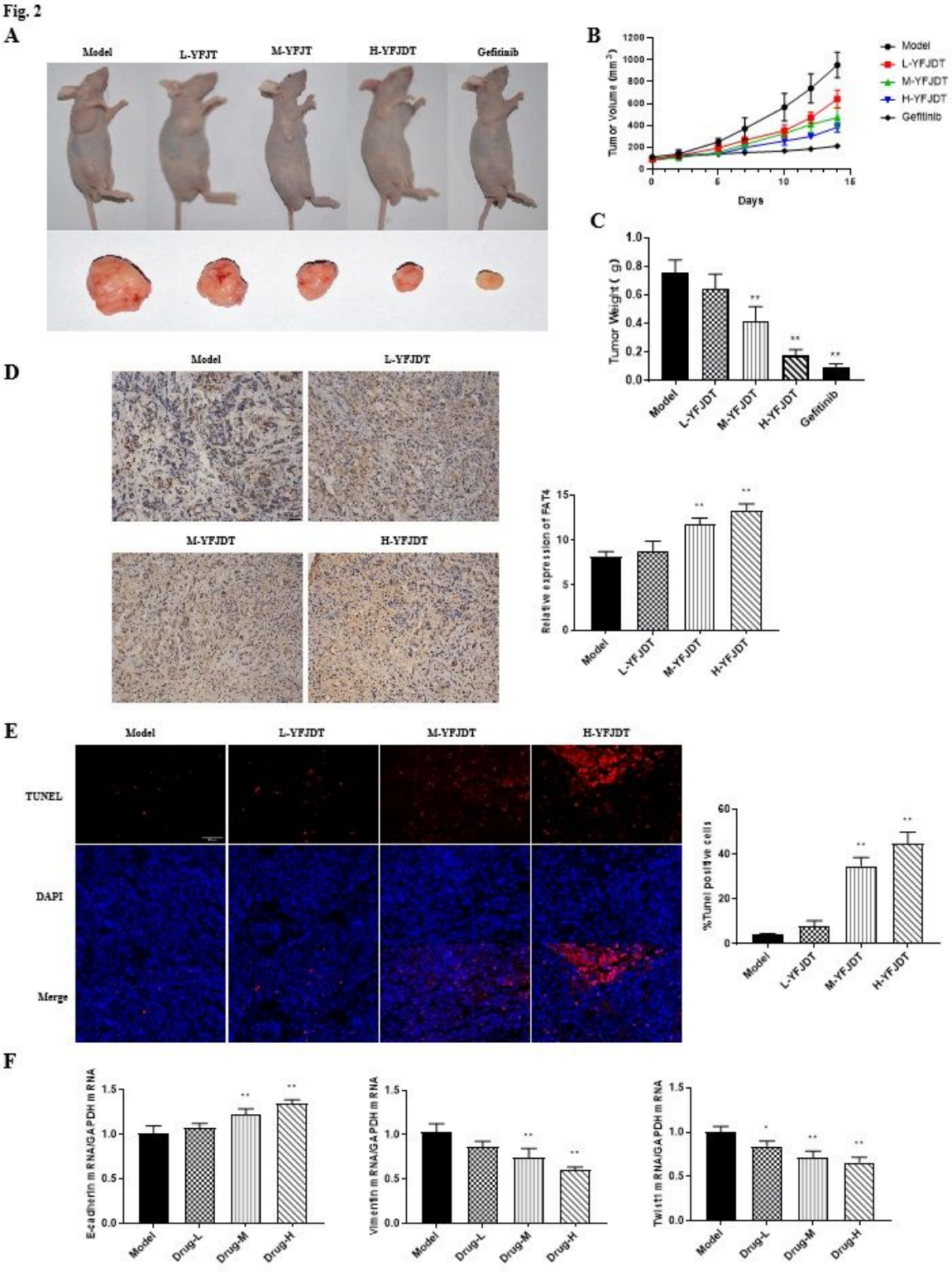

Figure 2

YFJDT reduces the volume and weight of tumor in mice. (A) The size of tumor in different group. (B) The volume of tumor in different group. (C) The weight of tumor in different group. (D) Representative immunofluorescence images of FAT4 in tumor tissue of different group. (E) The proportion of apoptosis in the tumor of different group. (F) The m RNA expressions of E-cadherin, Vimentin and Twist1. Data are

expressed as mean ± SD, *P < 0.05 was considered a significant difference compared with the Model group, **P < 0.01 was considered an extremely significant difference compared with the Model group.

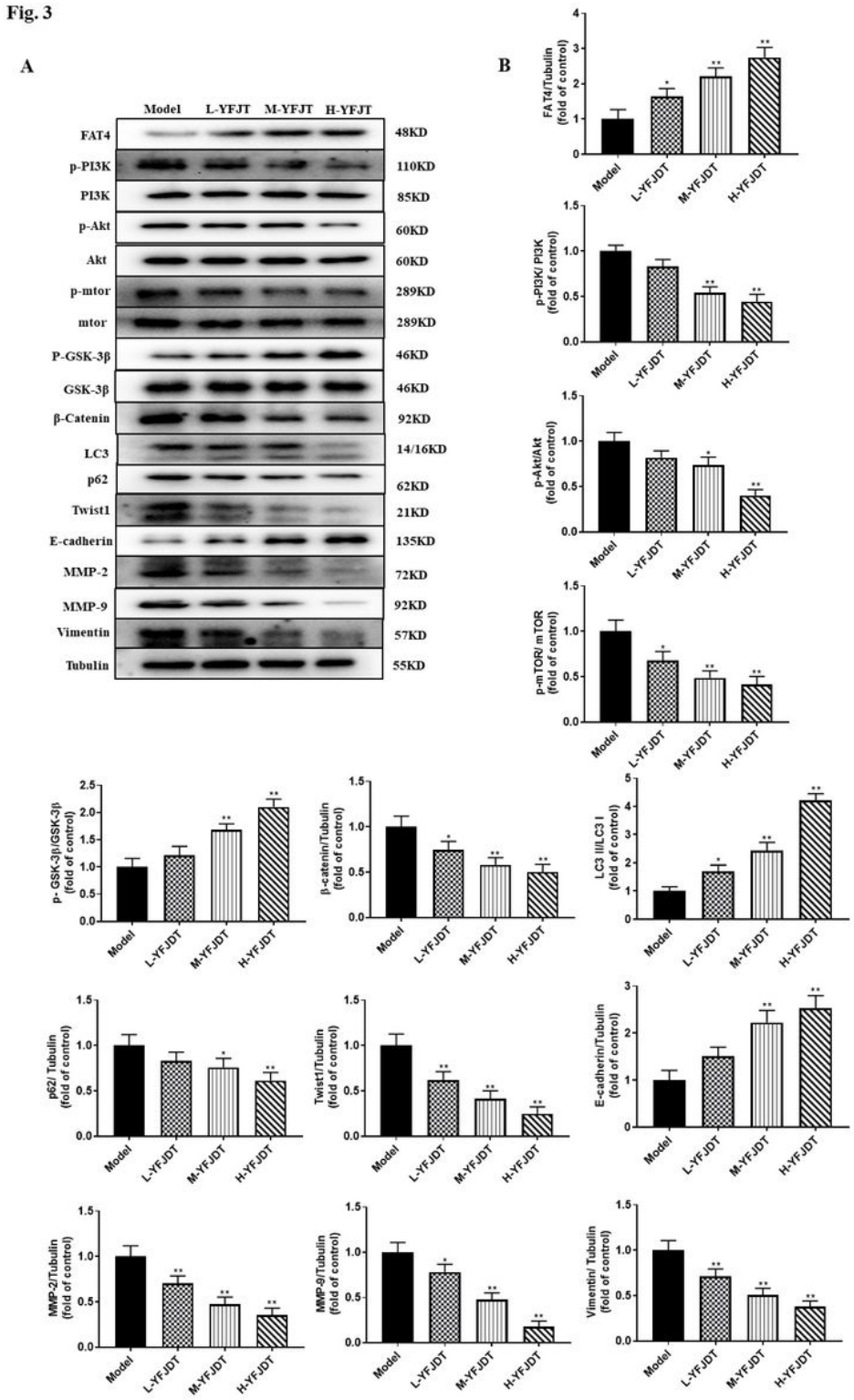

Figure 3

YFJDT promotes autophagy related proteins and inhibits migration proteins. (A) Western blot analysis of autophagy and migration related proteins. (B) Relative expressions of the indicated proteins normalized to levels of Tubulin. Data are expressed as mean ± SD, *P <0.05 was considered a significant difference

compared with the Model group, **P <0.01 was considered an extremely significant difference compared with the Model group.

Fig. 4

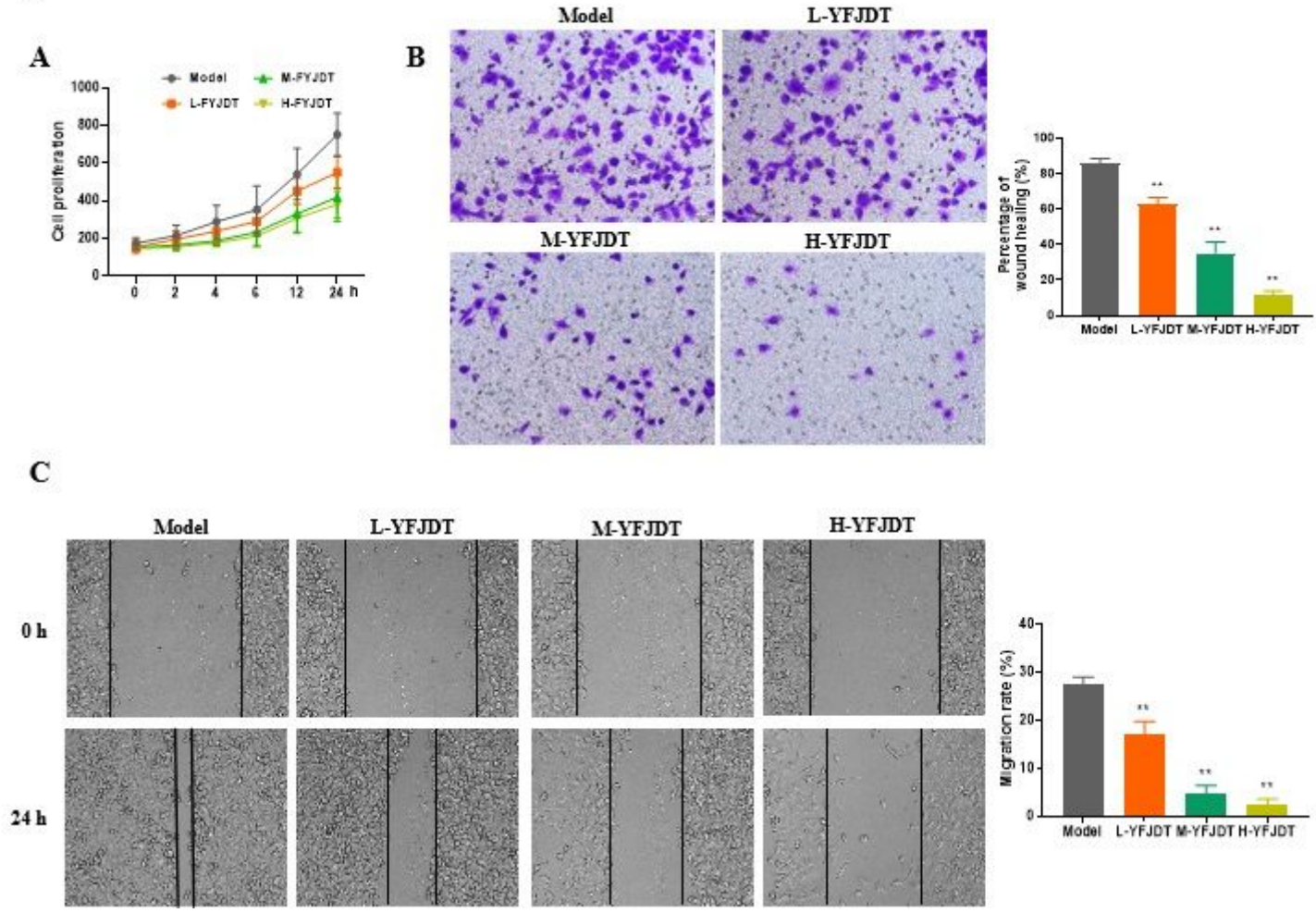

Figure 4

YFJDT-containing serum inhibits the proliferation of A549 cells. (A) The proliferation of A549 cells in each group. (B) The invasion of A549 cells in each group. (C) The migration of A549 cells in each group. Data are expressed as mean ± SD, *P < 0.05 was considered a significant difference compared with the Model group, **P < 0.01 was considered an extremely significant difference compared with the Model group.

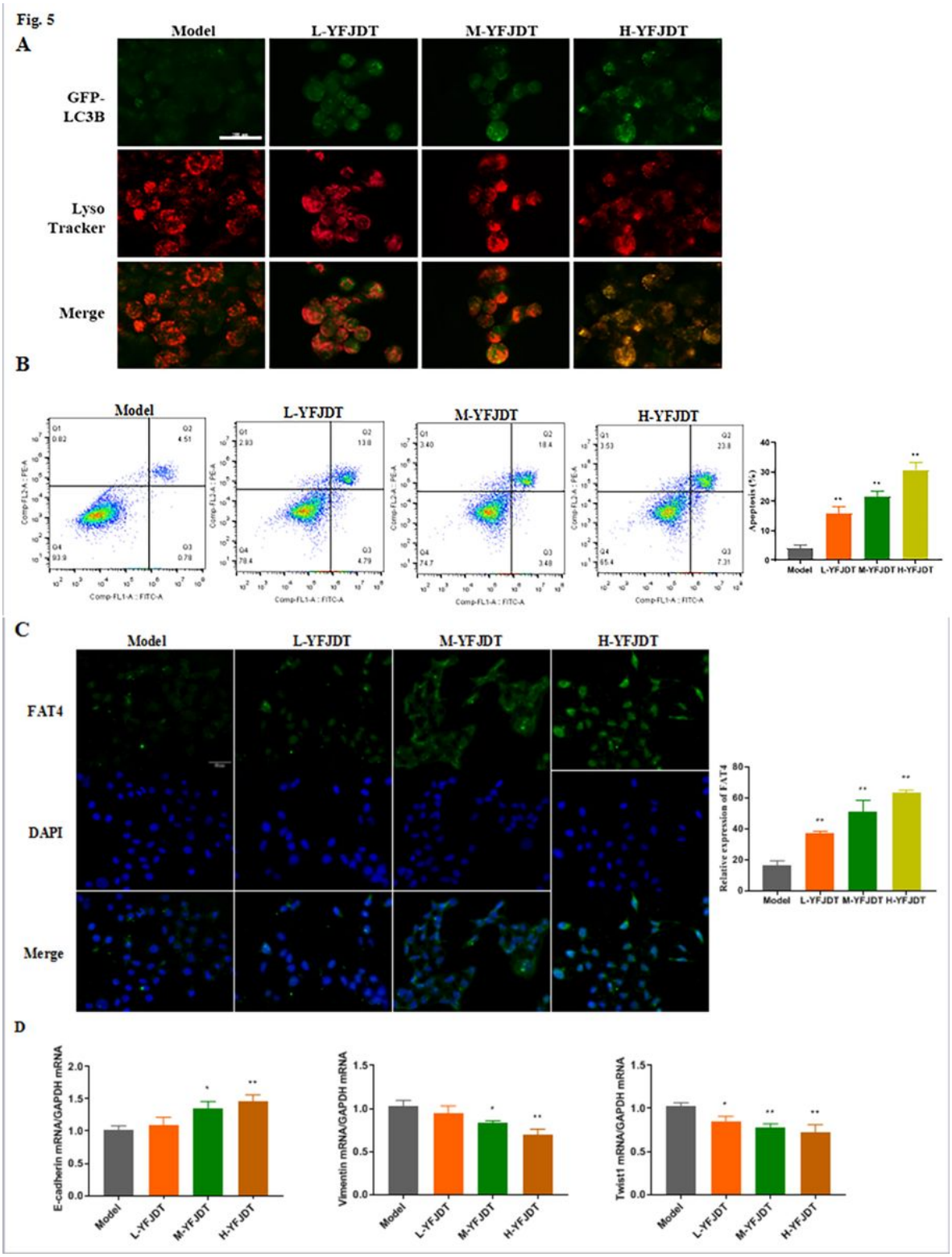

Figure 5

YFJDT increases the expressions of LC3 and FAT4 and the ratio of apoptosis. (A) The co-localization of GFP-LC3 with lysosomes in each group. (B) The apoptosis ratio in A549 cells in each group. (C) Representative immunofluorescence images of FAT4 of A549 cells in each group. (D) The mRNA expressions of E-cadherin, Vimentin and Twist1. Data are expressed as mean ± SD, *P < 0.05 was

considered a significant difference compared with the Model group, **P < 0.01 was considered an extremely significant difference compared with the Model group.

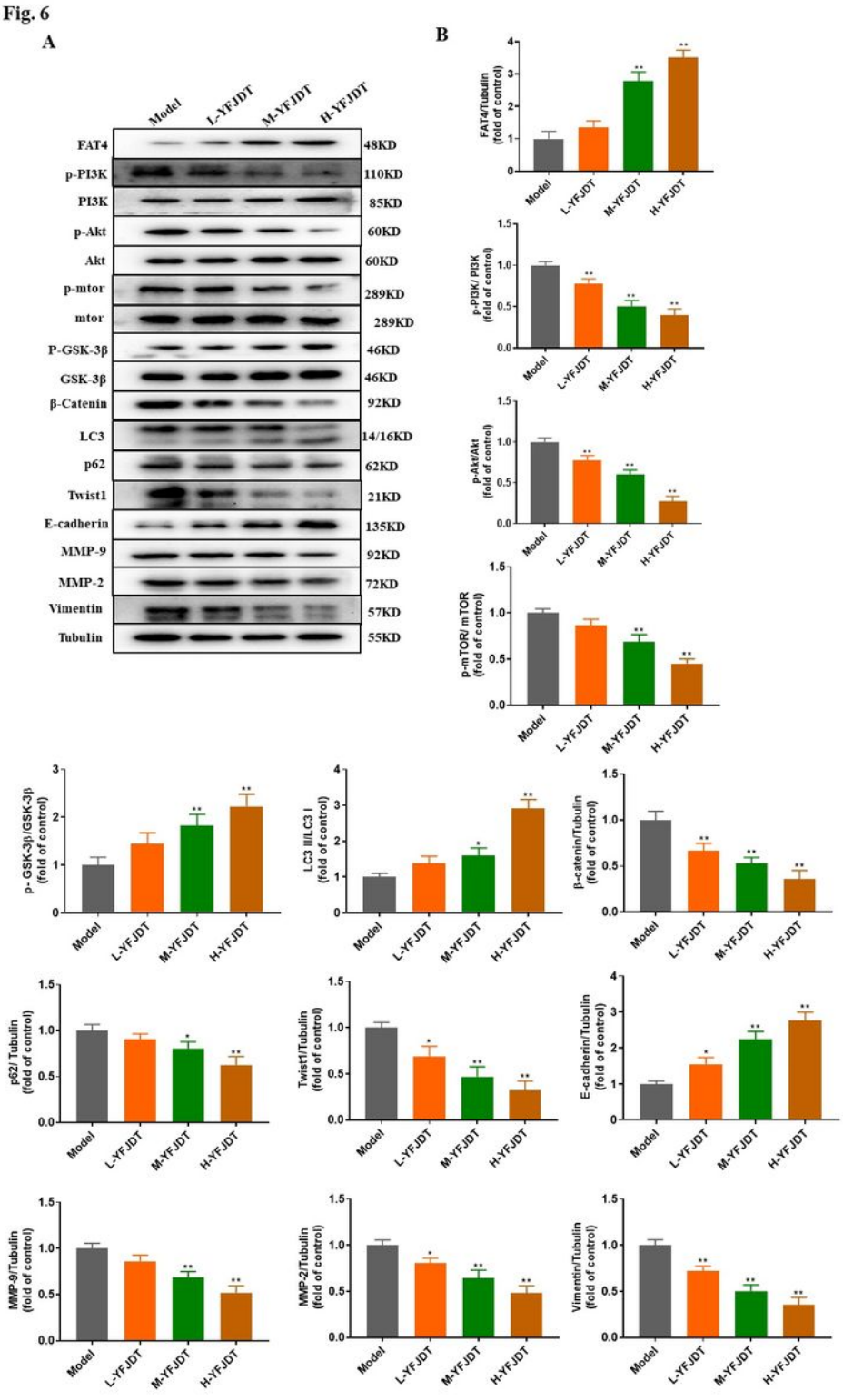

Figure 6

YFJDT promotes autophagy related proteins and inhibits migration proteins in A549 cells. (A) Western blot analysis of autophagy and migration related proteins in A549 cells. (B) Relative expressions of the indicated proteins normalized to levels of Tubulin. Data are expressed as mean ± SD, *P < 0.05 was

considered a significant difference compared with the Model group, **P < 0.01 was considered an extremely significant difference compared with the Model group.

Fig. 7

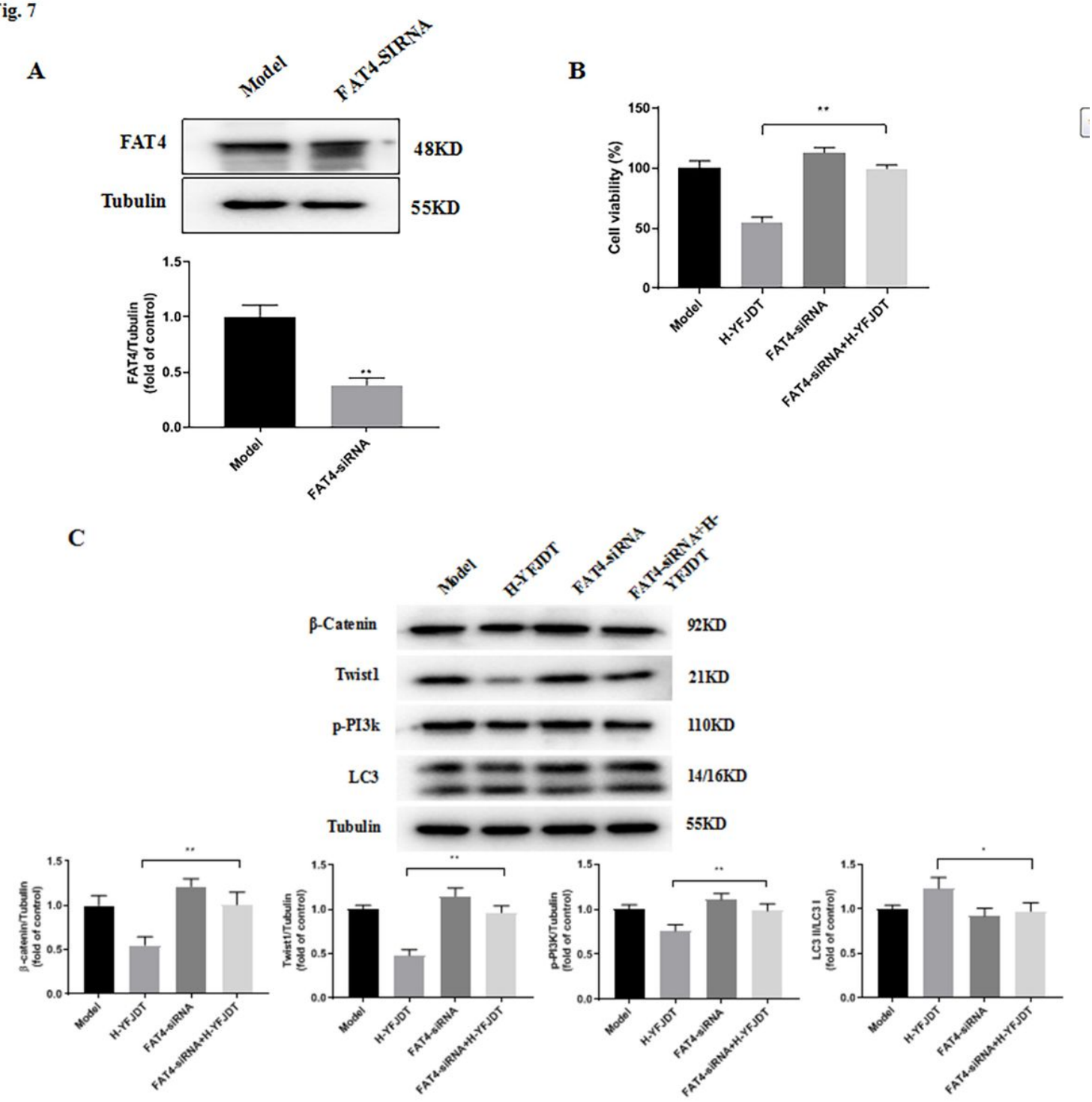

Figure 7

Si-FAT4 reduces the inhibition of YFJDT on the autophagy and migration of A549 cells. (A) The expression of FAT4 in A549 cells after treatment with FAT4 si-RNA. (B) The cell viability of A549 cells increased compared to that in the H-YFJDT group. (C) Western blot analysis of autophagy and migration

related proteins in A549 cells. Data are expressed as mean ± SD, *P<0.05 is considered significant and **P<0.01 is considered extremely significant.

Fig. 8

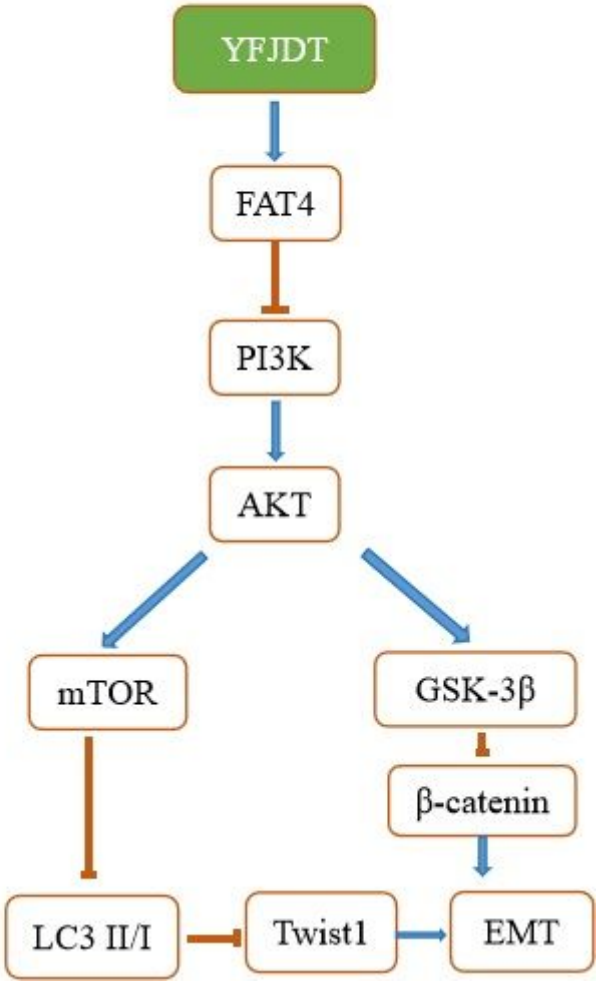

Figure 8

FAT4 can inhibit EMT by promoting autophagy and reducing Twist1 levels.